

Tuning Synaptic Connections instead of Weights by Genetic Algorithm in Spiking Policy Network

Duzhen Zhang^{1,2}, Tielin Zhang^{1,2*}, Shuncheng Jia^{1,2}, Qingyu Wang^{1,2} & Bo Xu^{1,2,3*}

¹Research Center for Brain-inspired Intelligence, Institute of Automation, Chinese Academy of Sciences, Beijing 100190, China;

²School of Artificial Intelligence, University of Chinese Academy of Sciences, Beijing 100049, China;

³Center for Excellence in Brain Science and Intelligence Technology, Chinese Academy of Sciences, Shanghai 200031, China

Abstract Learning from the interaction is the primary way biological agents know about the environment and themselves. Modern deep reinforcement learning (DRL) explores a computational approach to learning from interaction and has significantly progressed in solving various tasks. However, the powerful DRL is still far from biological agents in energy efficiency. Although the underlying mechanisms are not fully understood, we believe that the integration of spiking communication between neurons and biologically-plausible synaptic plasticity plays a prominent role. Following this biological intuition, we optimize a spiking policy network (SPN) by a genetic algorithm as an energy-efficient alternative to DRL. Our SPN mimics the sensorimotor neuron pathway of insects and communicates through event-based spikes. Inspired by biological research that the brain forms memories by forming new synaptic connections and rewires these connections based on new experiences, we tune the synaptic connections instead of weights in SPN to solve given tasks. Experimental results on several robotic control tasks show that our method can achieve the performance level of mainstream DRL methods and exhibit significantly higher energy efficiency.*

Keywords Spiking Neural Networks, Genetic Evolution, Bio-inspired Learning, Agent & Cognitive Architectures, Robotic Control

Citation Duzhen Zhang, Tielin Zhang, Shuncheng Jia, et al. Tuning Synaptic Connections instead of Weights by Genetic Algorithm in Spiking Policy Network. *Sci China Inf Sci*, for review

1 Introduction

When we think about the nature of learning, the idea of biological agents learning by interacting with their environment is probably the first thing that comes to mind. Reinforcement learning (RL) is an algorithm that attempts to study this biological mechanism of how biological agents learn from interaction from a computational perspective [1]. In RL, an artificial agent interacts with the environment in a trial-and-error manner and learns an optimal policy by maximizing accumulated rewards. In modern deep reinforcement learning (DRL), agents controlled by deep neural networks (DNNs) and optimized through gradient-based algorithms have proven to be capable of solving various tasks, from video games [2, 3] to robotic control [4, 5].

Despite remarkable progress, modern DRL suffers from high energy consumption, including high inference and optimization energy consumption, which has been a concern in real-world applications, especially for robot-control tasks with limited onboard energy resources [6]. Specifically, high inference energy consumption is because a deep policy network (DPN, a DNNs-based policy network) relies on the dense

* Corresponding author (email: tielin.zhang@ia.ac.cn, xubo@ia.ac.cn)

*The source code, saved checkpoints and results are available at <https://github.com/BladeDancer957/SPN-GA>.

communication of continuous floating-point values, suffering from high computational costs. High optimization energy consumption mainly comes from performing backpropagation (BP) [7]. For example, the computational cost of layer-by-layer BP for calculating gradients in gradient-based algorithms is hugely high, especially for optimizing parameters in a DPN by stochastic gradient descent/ascent.

In short, powerful as DRL is, it is still far from energy-efficient learning in biological agents. During learning from the interaction with the environment, biological agents typically exhibit ultra-low energy consumption [8–10]. Recent research has shown that the biological brain can perform complex calculations with only 20 watts of energy [11, 12]. The energy consumption existing computing systems require to achieve the same task is often at least an order of magnitude higher [13]. While it is still not completely understood how biological agents learn so efficiently, we believe that the integration of spiking communication between neurons and biologically-plausible synaptic plasticity plays a fundamental role.

Following this biological intuition, we optimize a spiking policy network (SPN) by using a gradient-free genetic algorithm (GA) as an energy-efficient alternative to DRL. Specifically, our SPN, used to infer actions from the state observations, draws inspiration from the biological sensorimotor neuron pathway found in insects [14, 15]. Neurons in the SPN communicate via event-based binary spikes, which can reduce inference energy consumption. To reduce optimization energy consumption, we design a gradient-free optimization paradigm based on GA, directly conducting SPNs search. Furthermore, in previous methods, optimizing a policy network is synonymous with tuning its synaptic weights. By contrast, we highlight the viewpoint of synaptic connection tuning. Inspired by biological research, the brain forms memories by forming new synaptic connections and rewires these connections based on new experiences [16–18], we only tune the synaptic connections of the SPN to solve given tasks without any synaptic weights tuning.

Our main contributions can be summarized as follow:

- Following biological intuition, we construct a biological-inspired SPN optimized by a gradient-free GA as an energy-efficient alternative to DRL.
- We highlight the viewpoint of synaptic connection tuning, that is, tuning synaptic connections instead of weights by GA in SPN to solve given tasks.
- Extensive experimental results on several robotic control tasks demonstrate that our alternative method can achieve the performance level of mainstream DRL methods and show significantly higher energy efficiency (save about 1.1~1.3 times inference energy consumption and 6.5~87.9 times optimization energy consumption under various tasks). Further analyses verify the superiority of connection tuning over weight tuning and the necessity of using GA to optimize SPN.

2 Related Work

2.1 RL

Conventional RL algorithms perform well on simple, tabular state spaces [1]. However, it is challenging for them to extract features from complex state space. Using DNNs as powerful function approximators, modern DRL has resolved this problem by directly learning a mapping function from the raw sensation state space to the action space. Two broad families of gradient-based algorithms typically optimize the DRL: the Q-learning algorithm [19] represented by DQN [2] and the policy gradient algorithm [20] represented by PPO [21].

DQN [2] approximates the optimal Q function using DNNs, resulting in a policy that chooses the action maximizing the Q-value for a given state. It contains two essential techniques: the experience replay and the target network. The former stores the agent’s experiences into a replay buffer and allows them to be used in many weight updates for greater data efficiency. The latter aims to generate the targets in the Q-learning update and address the instability problem of the combination between DNNs

and Q-learning. DQN and its improved variants, such as Double DQN [22] and Dueling DQN [23], are developing towards human-level control in Atari video games [24] with discrete action spaces.

However, the above value-based DRL algorithms can not take all scenarios due to insufficient processing capacity for the continuous action spaces. To remedy this defect, PG algorithm [20] is proposed to directly learn the parameters in a DPN, even though still suffering from the high variance problem, partly caused by the probabilistic output for taking actions. To reduce the gradient variance, the actor-critic (AC) framework is proposed, where a deep actor/policy network is used to infer an action from a given state, and a deep critic/value network is used to estimate the associated state-value or action-value to guide the actor to learn a better policy during the optimization. After that, numerous improved AC-based PG algorithms have been proposed for achieving better exploration and data efficiency, including A3C [25], TRPO [26], PPO [21], DDPG [5], TD3 [27], SAC [28], etc. Among these algorithms, PPO is easier to implement and more general, which can be scaled to almost all task scenarios, including video games with discrete action spaces and robotic control with discrete or continuous action spaces (The optimization process of PPO is shown in Appendix A).

Despite remarkable progress, the solutions found by the DRL algorithms described above are typically energy-intensive due to the DPN relying on dense communication of continuous values and the gradient-based optimization paradigm. To remedy this deficiency, we introduce a biologically-inspired SPN optimized by a gradient-free GA as an energy-efficient alternative to DRL.

2.2 Integrating Spiking Neural Networks (SNNs) with RL

Recently, the literature has grown around integrating SNNs [29,30] with RL. Early methods [31–35] are typically based on local plasticity rules such as reward-modulated spike-timing-dependent plasticity [36, 37]. They perform well in simple tasks, e.g., logic gate function and random walk problem [32], but fail in complex video games or robotic control due to limited optimization capability.

To address the limitation, some methods embed SNNs into gradient-based DRL optimization algorithms [38]. Based on the Q-learning algorithm, some methods train a deep spiking Q-networks directly [15,39–41] or convert the trained DQNs to SNNs [42,43], achieving competitive scores on Atari video games with discrete action space. Other methods propose a hybrid learning framework tested on robotic control tasks with continuous action space, where a population-coded spiking actor network is trained in conjunction with deep critic networks using AC-based PG algorithms like PPO [6,44–46]. Although the above methods can obtain a SNNs-based policy network for inference to solve DPN’s high inference energy consumption, they still rely on gradient-based optimization algorithms, with the high optimization energy consumption neglected.

2.3 Neuroscience

In neuroscience, a connectome [47] is the “wiring diagram”, mapping all the brain’s neural connections. At present, the connectome of simple organisms such as fruit flies [48,49] and roundworms [50,51] has been constructed. The motivation for studying the connectome is that it will help guide future research on how the brain learns and represents memories in its connections [52]. It is evident that biological agents such as humans form memories and learn skills by constructing new synaptic connections, especially during early childhood [53,54]. And their brain rewires these connections based on new experiences [16–18,55]. Inspired by the above biological research, we integrate biologically plausible synaptic connection tuning with biologically inspired SPN for energy-efficient robotic control.

3 Method

3.1 Constructing a SPN

In RL tasks, an artificial agent interacts with its environment via a series of state observations, actions, and rewards. At each time step t , with a given state observation \mathbf{o}^t , the agent selects action \mathbf{a}^t concerning

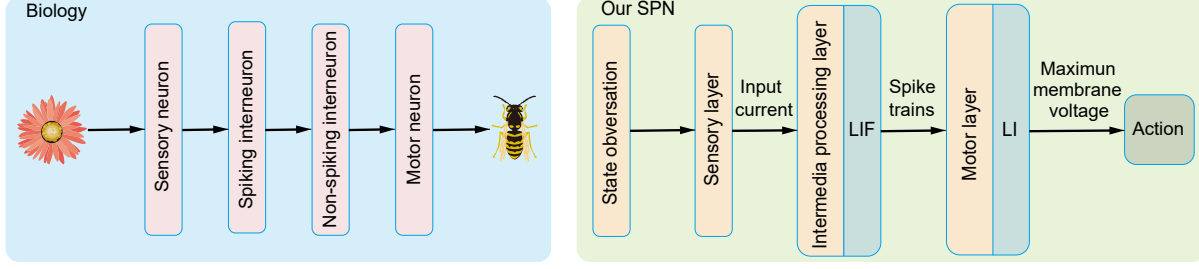


Figure 1 The correspondence diagram between the sensorimotor neuron pathway and our SPN.

a policy π , receiving a scalar reward r^{t+1} and the new state observation of the environment \mathbf{o}^{t+1} . This interaction produces an episode: $\epsilon = \{\mathbf{o}^0, \mathbf{a}^0, r^1, \dots, \mathbf{o}^{T-1}, \mathbf{a}^{T-1}, r^T\}$, where T is the length of ϵ . The return of the episode ϵ is defined as the sum of rewards $R^\epsilon = \sum_{i=1}^T r^i$. Here, we construct a SPN to represent the policy π , learning a mapping from state observations to actions, i.e., inferring actions \mathbf{a}^t from observations \mathbf{o}^t .

Our SPN draws inspiration from the biological sensorimotor neuron pathway found in insects [14, 15]. In this pathway, sensory neurons receive information from the external environment and transmit it to spiking interneurons with discrete dynamics. When the afferent current causes the membrane potential of the spiking interneurons to exceed a certain threshold, they generate spikes. Then, the spikes transmit the signals to non-spiking interneurons, whose membrane potential determines the input current of motor neurons for effective locomotion.

To correspond to this biological pathway, our SPN contains a three-layer architecture of sensory, middle processing, and motor. The correspondence diagram between the sensorimotor neuron pathway and our SPN is shown in Figure 1. Taking the robotic control task as an example, the sensory layer receives a continuous state observation $\mathbf{o} \in \mathbb{R}^n$, including information such as the angles, velocities, and external forces of each joint of the simulated robot, where n is the dimension of the input observation. Then the observation is transmitted to the middle processing layer. The neurons of the middle processing layer are implemented with the leaky integrate-and-fire (LIF) [56], the most commonly used artificial spiking neuron. And the neurons of the motor layer are implemented with the leaky integrate (LI) [15], a non-spiking neuron similar to LIF but without firing and resetting. Next, we describe the basic neuron models of our SPN in detail.

LIF. The dynamic firing process at neuron j can be described as:

$$\begin{cases} \frac{dv_{j,\tau}}{d\tau} = -g(v_{j,\tau} - v_{rest}) + \sum_{i=1}^n (w_{i,j} \times x_{i,j}) o_{i,\tau} \\ v_{j,\tau} = v_{reset}, s_{j,\tau} = 1 \quad \text{if } (v_{j,\tau} > v_{th}) \end{cases} \quad (1)$$

where $j = 1, \dots, h$, h is the number of neurons in the middle layer, $\tau = 1, \dots, T'$, τ is a simulation time step, T' is the number of simulation time step (i.e., time window), meaning the same observation will be fed into SPN for T' times, $v_{j,\tau}$ is the membrane potential, g is the decay factor, v_{rest} denotes the rest membrane potential, $s_{j,\tau}$ means the output spike, $x_{i,j}$ is a binary variable indicating whether the synaptic connection from neuron i to j exists, $o_{i,\tau}$ is the input current from upstream neuron i ($i = 1, \dots, n$), v_{th} is the predefined firing threshold, v_{reset} denotes the predefined reset membrane potential, and $w_{i,j}$ is the synaptic weight between neuron i and j . In our method, we only tune synaptic connections instead of weights (See Section 3.2 for details).

As shown in equation (1), the LIF neuron mimics the biological neuron by incorporating a time dimension τ , simulating the change in membrane potential over time. Due to the threshold firing characteristic of the LIF neurons, the spike signal is typically sparse. And the calculation is driven by events (i.e., only executed when the spike arrives), which can reduce the inference energy consumption especially deployed on neuromorphic chips [57, 58].

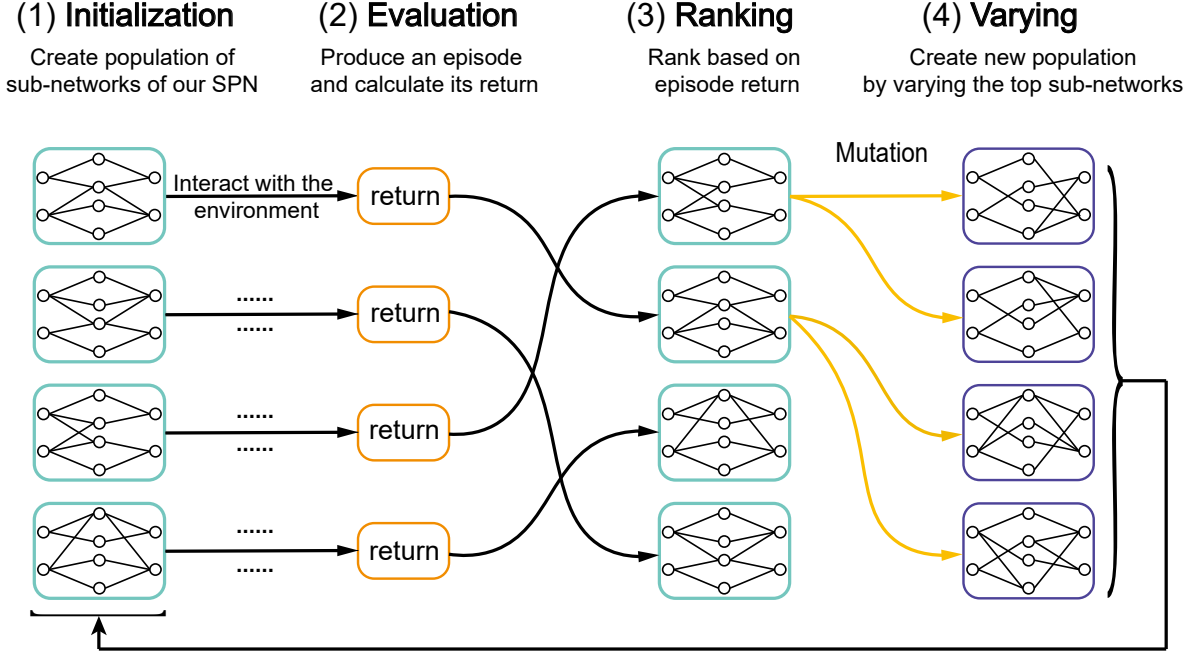


Figure 2 Overview of the evolution of our SPN sub-networks.

LI. The LI neuron can be regarded as a special case of LIF neuron without firing and resetting. If we set the firing threshold v_{th} of a LIF neuron to infinity, its dynamics will always be below the threshold, so-called non-spiking neurons. The dynamic equation (1) can be simplified to:

$$\frac{dv_{k,\tau}}{d\tau} = -g(v_{k,\tau} - v_{rest}) + \sum_{j=1}^h (w_{j,k} \times x_{j,k}) s_{j,\tau} \quad (2)$$

where $k = 1, \dots, m$ and m is the number of neurons in the motor layer.

The LI neurons serve as a spike decoder to convert spike trains from the previous layer to continuous values. With the recording membrane potential of LI neurons $\mathbf{v}_\tau \in \mathbb{R}^m$ at each simulation time step τ , we compute the maximum membrane potential to generate the output action:

$$\begin{cases} \mathbf{a} = \max_{1 \leq \tau \leq T'} \mathbf{v}_\tau, \text{ continuous action space} \\ \mathbf{a} = \arg \max(\max_{1 \leq \tau \leq T'} \mathbf{v}_\tau), \text{ discrete action space} \end{cases} \quad (3)$$

where $\mathbf{a} \in \mathbb{R}^m$ denotes the torque applied to each joint of the robot for continuous action space, and a denotes one of the predefined actions for discrete action space. The forward inference pseudocode of our SPN is summarized in Appendix B.

3.2 Tuning Synaptic Connections by GA

For an artificial agent in a simulation environment, our method aims to evolve the sub-networks of the SPN to solve a given task. During this process, we only tune the synaptic connections by GA, deemphasizing tuning of synaptic weights. The evolution of the sub-networks of our SPN can be summarized as follows (see Figure 2 for an overview):

Initialization We initialize the first generation population \mathcal{P}^0 of N individuals, each of which represents a vector of SPN parameters θ_j^i . It only contains scores corresponding to all synaptic connections without synaptic weights (randomly initialized and fixed). To reduce variance, we use mirrored sampling

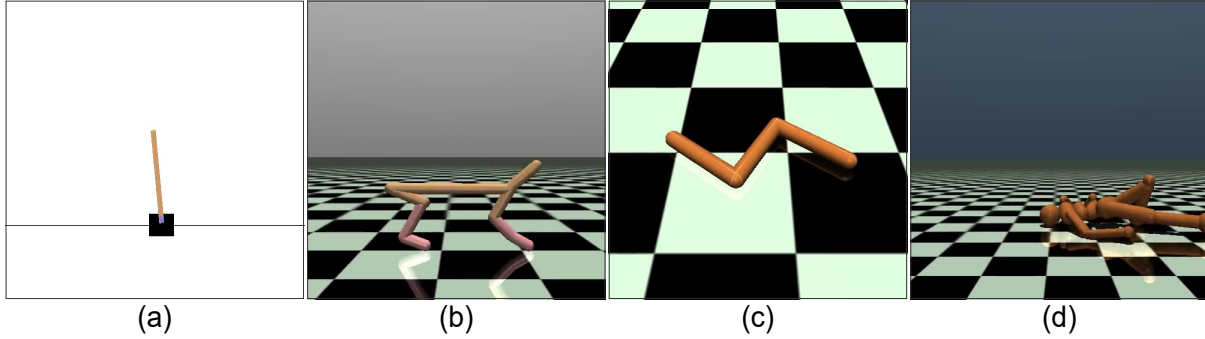


Figure 3 Four robotic control tasks. (a) **CartPole-v1**: Observation dimension: $n = 4$, Action dimension: $m = 2$ (discrete), Goal: balance a pole on a cart; (b) **HalfCheetah-v2**: Observation dimension: $n = 17$, Action dimension: $m = 6$ (continuous), Goal: make a 2D cheetah robot run as fast as possible; (c) **Swimmer-v2**: Observation dimension: $n = 8$, Action dimension: $m = 2$ (continuous), Goal: make a 2D robot swim; (d) **HumanoidStandup-v2**: Observation dimension: $n = 376$, Action dimension: $m = 17$ (continuous), Goal: make a 3D two-legged robot standup.

from previous evolution strategy literature [59–61], i.e., always using pairs of perturbations to produce individuals: $\theta_j^0 = \sigma\epsilon$ or $-\sigma\epsilon$, where $j = 0, \dots, N-1$, σ is the standard deviation, $\epsilon \sim \mathcal{N}(\mathbf{0}, \mathbf{I})$. After that, we normalize the connection scores between 0 and 1 by the sigmoid function and then set a score threshold of s_{th} , if the normalized score is less than s_{th} , remove the connection, otherwise keep the connection, obtaining a sub-network. It can be considered that each SPN sub-network corresponds to an individual.

Evaluation At every generation i , where $i = 0, \dots, G-1$ and G is the number of total generations, each sub-network is evaluated to produce a fitness score. Based on the interaction between the sub-network and the environment, we can obtain an episode and use its return as the fitness score.

Ranking We rank each sub-network in descending order according to fitness. We perform truncation selection with a ratio of η , i.e., the top $(\eta * 100)\%$ of sub-networks will be the next generation’s parents, denoted as \mathcal{P}_η^i . To more reliably obtain the optimal sub-network, we evaluate each of the top 10 sub-networks of each generation in 10 additional episodes (counting these interaction steps as ones consumed during optimization). The one with the highest average return is called the “elite” sub-network of the current generation.

Varying Next generation population \mathcal{P}^{i+1} of N sub-networks is created by varying the parents obtained via truncation selection in the previous step. This process of variability is typically called “Mutation”. Specifically, we produce offsprings by adding the perturbation generated by mirror sampling to the parents: $\theta_j^{i+1} = \theta_{j_n}^i + \sigma\epsilon$ or $-\sigma\epsilon$, where $j = 0, \dots, N-1$, and $\theta_{j_n}^i \in \mathcal{P}_\eta^i$ is selected uniformly at random with replacement. We can get new sub-networks (individuals) by sigmoid normalization of connection scores and filtering by the score threshold s_{th} . Steps **Evaluation-Varying** can be repeated $G-1$ times.

The pseudocode for our GA version is summarized in Appendix C.

4 Experimental Settings

4.1 Evaluation Tasks

As shown in Figure 3, we evaluated our method on a benchmark of robotic control tasks interfaced by OpenAI Gym [62]. They included classic discrete control, like CartPole-v1, and more difficult continuous control, like HalfCheetah-v2, Swimmer-v2, and HumanoidStandup-v2 running in the fast physics simulator MuJoCo [63]. Without modifying the environment or reward manually, the original CartPole-v1 task had an upper limit return of 500.

4.2 Implement Details

On all tasks, our SPN was a multi-layer perceptron architecture with a 64-unit middle layer, i.e., (sensory layer, middle processing layer, LIF, motor layer, LI), where the number of simulation time step T' was 4, the decay factor g was 0.75, the rest and reset potential v_{rest} and v_{reset} were both 0, and the firing threshold v_{th} was 0.5. In our GA version, we set the number of generations G to 100, the number of individuals N in each generation to 200, the standard deviation σ of perturbations to 0.01, the ratio η of truncation selection to 0.25, and the connection score threshold s_{th} to 0.5.

For a fair comparison, on all tasks, the DPN was set up with the same number of parameters and architecture as our SPN but with different neuron types, i.e., (sensory layer, middle processing layer, ReLU, motor layer, Tanh). It was optimized in conjunction with a deep value network by PPO [21] (one of the most general RL algorithms and the default RL algorithm at OpenAI). The architecture of the deep value network was (sensory layer, middle processing layer, ReLU, output layer), where the output layer with 1 unit estimated the value of the input observation. The PPO implementation and its hyper-parameter configurations were from OpenAI Spinning Up [64]. Our DPN baseline achieved similar or better performance than reported in the literature [21, 65]. The hyper-parameter configurations and optimization process of PPO were shown in Appendix A.

Due to recent concerns in reproducibility [66], we used the original set of tasks from Gym [62] with no modifications to the reward or environment. We performed 10 independent runs (with different random seeds) for all experiments. In GA, we ran each task for 100 generations and evaluated each generation’s “elite” sub-network with 10 episodes, and reported the average return over 10 runs. In PPO, following previous works [21, 65], we ran each task for $1e6$ steps and evaluated the final learned DPN with 10 episodes, and reported the average return over 10 runs as its performance level. All of the experiments were conducted on an AMD EPYC 7742 server.

5 Results and Discussions

The goals of our experiments were the following:

1. To demonstrate the feasibility of our alternative method, tuning the synaptic connections of SPN by gradient-free GA (SPN-Connections-GA), when compared to the mainstream DRL method, tuning the synaptic weights of DPN by gradient-based PPO (DPN-Weights-PPO) (Section 5.1);
2. To demonstrate the superiority of connection tuning over weight tuning (Section 5.2);
3. To demonstrate the necessity of using GA to optimize SPN (Section 5.3);
4. To demonstrate the dynamic evolution process of SPN-Connections-GA (Section 5.4).

5.1 SPN-Connections-GA vs. DPN-Weights-PPO

In this section, we compared our alternative method: SPN-Connections-GA, with the mainstream DRL method: DPN-Weights-PPO, in terms of return gained, data efficiency, and energy efficiency.

5.1.1 Return Gained

As shown in Figure 4 (a), on the classical discrete control task CartPole-v1, SPN-Connections-GA reached the upper limit return of 500, preliminarily verifying the feasibility of our method. As shown in Figure 4 (b) – (d), on more difficult MuJoCo continuous control tasks HalfCheetah-v2, Swimmer-v2, and HumanoidStandup-v2, our SPN-Connections-GA was able to achieve the performance level of DPN-Weights-PPO (the red horizontal line in the figure).

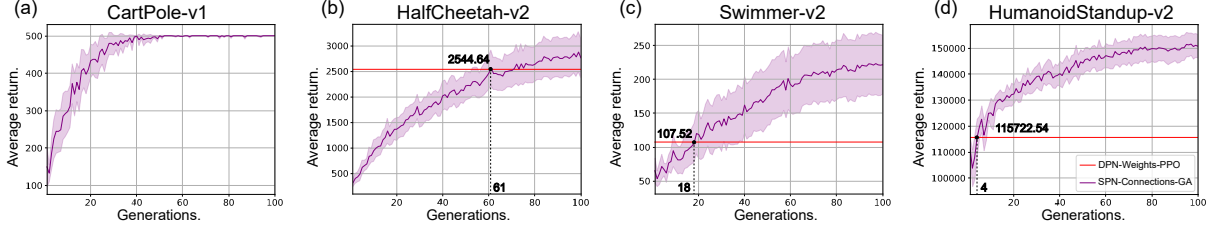


Figure 4 Learning curves for the OpenAI Gym robotic control tasks. The purple areas represented the learning curves of SPN-Connections-GA during 100 generations of evolution, where the solid curves correspond to the mean and the shaded region to half a standard deviation over 10 runs. The red horizontal line represented the performance level of DPN-Weights-PPO.

Table 1 The exact data efficiency tradeoffs between SPN-Connections-GA and DPN-Weights-PPO. \mathcal{R} denoted the performance level of DPN-Weights-PPO after using $1e6$ steps of environment interaction. γ denoted a measure of data efficiency, defined in Equation (4).

Task	\mathcal{R}	\mathcal{G}	\mathcal{E}	γ
HalfCheetah-v2	2544.64	61	$1.83e7$	18.3
Swimmer-v2	107.52	18	$5.4e6$	5.4
HumanoidStandup-v2	115722.54	4	$1.2e6$	1.2

5.1.2 Data Efficiency

As we all know, the data efficiency of GA was typically low. In our SPN-Connections-GA, each data (step) that interacted with the environment was used only once. However, we found that its data efficiency γ was surprisingly good. As Table 1 shows, using no more than 18.3x as much data (18.3x on HalfCheetah-v2, 5.4x on Swimmer-v2, and 1.2x on HumanoidStandup-v2), our SPN-Connections-GA was able to achieve the performance level of DPN-Weights-PPO, which used $1e6$ steps of environment interaction. DPN-Weights-PPO was more data-efficient because it maintained a vast replay buffer for storing data interacting with the environment. Data in the buffer was utilized multiple times during optimization. Due to not using data repeatedly, not having a deep value network, and not performing BP during optimization, the energy consumption of our SPN-Connections-GA was much lower, which offset the slight decrease in data efficiency. The specific data efficiency calculation method was defined as follows.

For each MuJoCo control task, we first calculate the steps \mathcal{E} of environment interaction required for SPN-Connections-GA to achieve the performance level \mathcal{R} of DPN-Weights-PPO. Then, we calculate the ratio γ of \mathcal{E} to standard PPO steps ($1e6$) as a measure of data efficiency.

$$\begin{aligned}
 \mathcal{A} &= N \times T + 10 \times 10 \times T \\
 \mathcal{E} &= \mathcal{G} \times \mathcal{A} \\
 \gamma &= \mathcal{E}/1e6
 \end{aligned} \tag{4}$$

where \mathcal{G} was the number of generations required to achieve the performance level of DPN-Weights-PPO (inferred from the vertical dashed line in Figure 4 (b) – (d)), \mathcal{A} denoted the number of interaction steps consumed per generation of optimization, T was the length of the episode ($T=1000$ in all the tasks we used), and $N=200$ was the number of individuals in each generation (each individual needed to interact with the environment to get an episode and use the return of the episode as its fitness score). In each generation, we needed to evaluate each of the top 10 individuals in 10 additional episodes to obtain the “elite” individual. Thus, \mathcal{A} was $3e5$. The exact data efficiency tradeoffs were listed in Table 1.

5.1.3 Energy Efficiency

In this part, we analyzed the energy efficiency of our SPN-Connections-GA with the DPN-Weights-PPO from inference and optimization. As shown in Table 2, our SPN’s network inference energy consumption

Table 2 The network inference energy consumption comparison of our SPN and DPN. The input layer in our SPN was non-spiking, so it's energy was same as DPN. Unit: pJ.

Task	E_{DPN}^{infer}	E_{SPN}^{infer}	$\frac{E_{DPN}^{infer}}{E_{SPN}^{infer}}$
HalfCheetah-v2	6.77e3	5.2e3	1.3
Swimmer-v2	2.94e3	2.41e3	1.2
HumanoidStandup-v2	1.16e5	1.1e5	1.1

Table 3 The optimization energy consumption comparison of our GA and PPO. Unit: pJ

Task	E_{PPO}^{optim}	E_{GA}^{optim}	$\frac{E_{PPO}^{optim}}{E_{GA}^{optim}}$
HalfCheetah-v2	6.16e11	9.52e10	6.5
Swimmer-v2	2.85e11	1.3e10	21.9
HumanoidStandup-v2	1.16e13	1.32e11	87.9

saves 1.3, 1.2, and 1.1 times of energy on HalfCheetah-v2, Swimmer-v2, and HumanoidStandup-v2, respectively, compared to DPN. As shown in Table 3, our GA's optimization energy consumption saves 6.5, 21.9, and 87.9 times of energy on HalfCheetah-v2, Swimmer-v2, and HumanoidStandup-v2, respectively, compared to PPO. The specific energy consumption calculation method was defined as follows.

For inference, we first analyzed the computing patterns of DPN and SPN. For DPN, each operation calculated a dot-product containing one floating-point multiplication and one accumulation (MAC), whereas, for SPN, each operation was only one accumulation (AC) due to binary spikes (0 or 1). The computations in SPN deployed on neuromorphic hardware [58] were event-driven (i.e., only executed when the spike arrives). Following [67], we computed the inference energy consumption for DPN and SPN in 45nm CMOS technology. Previous literature showed that the energy consumption for 32-bit DNN MAC operation ($e_{MAC}=4.6pJ$) is $5.1\times$ more than SNN AC operation ($e_{AC}=0.9pJ$) [68].

Following [67], in DPN, we defined the number of operations at layer l as:

$$\#OP_{DPN} = f_{in} \times f_{out} \quad (5)$$

where $f_{in}(f_{out})$ was the dimension of input (output) features at layer l . The number of operations at layer l in SPN was defined as:

$$\begin{aligned} \#OP_{SPN} &= rate_l \times \#OP_{DPN} \\ rate_l &= \frac{\#totalSpikes_l}{\#n_l} \end{aligned} \quad (6)$$

where $rate_l$ was the total spikes at layer l over time window averaged over the number of neurons n_l at layer l (averaged over all interaction steps). We defined the network inference energy consumption as:

$$\begin{aligned} E_{DPN}^{infer} &= \sum_l \#OP_{DPN} \times e_{MAC} \\ E_{SPN}^{infer} &= \sum_l \#OP_{SPN} \times e_{AC} \end{aligned} \quad (7)$$

We defined optimization energy consumption as the network inference energy consumption multiplied by the number of network inferences during optimization:

$$\begin{aligned} E_{PPO}^{optim} &= E_{DPN}^{infer} \times (N_{DPN}^{forward} + N_{DPN}^{backward}) \\ &\quad + E_{DVN}^{infer} \times (N_{DVN}^{forward} + N_{DVN}^{backward}) \\ E_{GA}^{optim} &= E_{SPN}^{infer} \times N_{SPN}^{forward} \end{aligned} \quad (8)$$

Note that the PPO optimization process included the forward inference and backpropagation of the DPN, and the forward inference and backpropagation of the deep value network (DVN) (The inference energy consumption calculation of DVN E_{DVN}^{infer} is similar to that of DPN E_{DPN}^{infer}). For simplicity, we

Table 4 The specific forward and back propagation times of data in the network.

		Policy Network		Value Network	
		forward	backward	forward	backward
PPO		2.6e7	2.5e7	2.6e7	2.5e7
GA	HalfCheetah	1.83e7	–	–	–
	Swimmer	5.4e6	–	–	–
	HumanoidStandup	1.2e6	–	–	–

considered the network backpropagation and forward inference to be the same energy consumption. Specifically, for each task, during PPO optimization, it needed to interact with the environment to collect a total of $1e6$ data (steps). Each time a piece of data was collected, DPN (inferred an action based on observation) and DVN (estimated the value of the observation) both needed to forward inference once. For every $1e3$ data collected, 25 epochs of optimization (including forward inference and backpropagation of DPN and DVN) would be conducted based on these data. During GA optimization, there was only forward inference of SPN. The number of forward inferences corresponded to the number of data (i.e., $N_{SPN}^{forward}$ in Equation (8) equaled \mathcal{E} in Equation (4)). The forward and backpropagation times of data in the network were listed in Table 4. Note that we calculated the optimization energy of our SPN-Connections-GA when achieving the performance level of the DPN-Weights-PPO.

5.2 SPN-Connections-GA vs. SPN-Weights-GA

In this section, we verified the superiority of connection tuning over weight tuning by comparing the performance of SPN-Connections-GA with SPN-Weights-GA.

As shown in Figure 5 (a) – (c), compared with SPN-Weights-GA, SPN-Connections-GA achieved a higher average return on HalfCheetah-v2 and Swimmer-v2 and achieved comparable average return on HumanoidStandup-v2. Moreover, after 100 generations of evolution, SPN-Weights-GA could not achieve the performance level of DPN-Weights-PPO on HalfCheetah-v2 and Swimmer-v2. Especially for Swimmer-v2, SPN-Weights-GA could hardly learn, and its performance had been kept at a shallow level. These results showed that SPN’s “elite” sub-network with random weights achieved a comparable or better return than the full-network with learned weights tuned by the same GA.

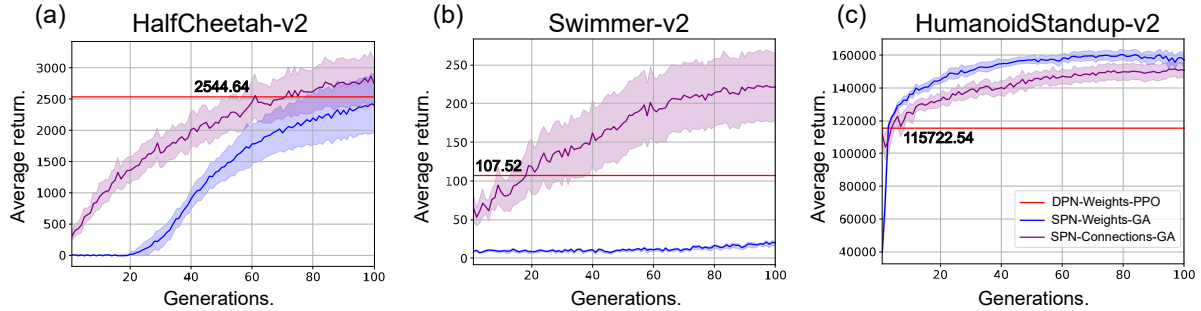


Figure 5 Learning curves for the MuJoCo continuous control tasks. The purple areas represented the learning curves of SPN-Connections-GA during 100 generations of evolution, where the solid curves correspond to the mean and the shaded region to half a standard deviation over 10 runs. The blue areas represented the learning curves of SPN-Weights-GA during 100 generations of evolution, where the solid curves correspond to the mean and the shaded region to half a standard deviation over 10 runs. The red horizontal line represented the performance level of DPN-Weights-PPO.

5.3 SPN-Connections-GA vs. SPN-Connections-PPO

In this section, we verified the necessity of GA to optimize SPN by benchmarking SPN-Connections-GA’s performance against SPN-Connections-PPO. We found that directly replacing DPN with our SPN and

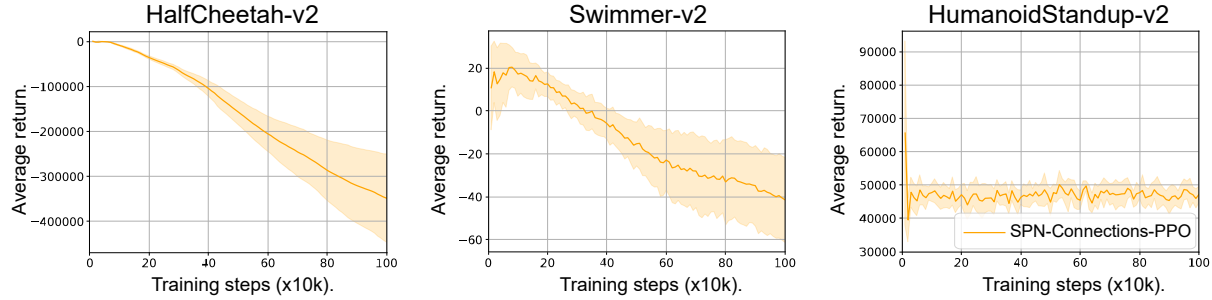


Figure 6 Learning curves for the MuJoCo continuous control tasks. The yellow areas represented the learning curves of SPN-Connections-PPO, where the solid curves correspond to the mean and the shaded region to half a standard deviation over 10 runs.

embedding it into the gradient-based PPO optimization framework did not work. As Figure 6 showed, the learning curve of SPN-Connections-PPO could hardly converge, and even its average return became lower and lower with the training. However, as shown in Figure 4, the SPN-Connections-GA learned well on these tasks. The poor performance of SPN-Connections-PPO might be because our SPN based on discrete spike communication was a low-precision network. When optimizing such a network, biased low-precision gradient estimates could be a problem when using a gradient-based PPO algorithm. Black-box optimization algorithms like GA might be uniquely suited to such a low-precision network.

5.4 The evolution process of SPN-Connections-GA

For MoJoCo continuous control tasks HalfCheetah-v2 and Swimmer-v2, we randomly sampled one of 10 independent evolutionary runs and visualized the dynamic evolution process of the sub-network of SPN. The video URLs of dynamic evolution were listed in Table 5.

Table 5 The video URLs of dynamic evolution.

Task	URL
HalfCheetah-v2	https://www.youtube.com/watch?v=_o0v3LtmU-U
Swimmer-v2	https://www.youtube.com/watch?v=JmxR4deP4Cc

6 Conclusion

In this paper, we optimize a biological-inspired SPN by a gradient-free GA as an energy-efficiency alternative to DRL. From a new perspective, we only tune synaptic connections instead of weights as in most previous methods, evolving “elite” sub-networks of the SPN to solve given tasks. Extensive experiments on several challenging robotic control tasks show that our method can achieve the performance level of mainstream DRL methods and shows significantly higher energy efficiency. Further analyses verify the superiority of connection tuning over weight tuning and the necessity of using GA to optimize SPN.

Acknowledgements This work was funded by the Strategic Priority Research Program of the Chinese Academy of Sciences (XDA27010404, XDB32070100), the Shanghai Municipal Science and Technology Major Project (2021SHZDZX), and the Youth Innovation Promotion Association CAS.

References

- Sutton R S, Barto A G. Reinforcement learning: An introduction[M]. MIT press, 2018.
- Mnih V, Kavukcuoglu K, Silver D, et al. Human-level control through deep reinforcement learning[J]. *nature*, 2015, 518(7540): 529-533.
- Vinyals O, Babuschkin I, Czarnecki W M, et al. Grandmaster level in StarCraft II using multi-agent reinforcement learning[J]. *Nature*, 2019, 575(7782): 350-354.

- 4 Duan Y, Chen X, Houthoofd R, et al. Benchmarking deep reinforcement learning for continuous control[C]//International conference on machine learning. PMLR, 2016: 1329-1338.
- 5 Lillicrap T P, Hunt J J, Pritzel A, et al. Continuous control with deep reinforcement learning[C]//ICLR (Poster). 2016.
- 6 Tang G, Kumar N, Yoo R, et al. Deep reinforcement learning with population-coded spiking neural network for continuous control[C]//Conference on Robot Learning. PMLR, 2021: 2016-2029.
- 7 Rumelhart D E, Hinton G E, Williams R J. Learning representations by back-propagating errors[J]. *nature*, 1986, 323(6088): 533-536.
- 8 Salem M S Z. Biological networks: an introductory review[J]. *Journal Of Proteomics And Genomics Research*, 2018, 2(1): 41-111.
- 9 Blanchini F, Franco E. Structurally robust biological networks[J]. *BMC systems biology*, 2011, 5(1): 1-14.
- 10 Whitacre J M. Biological robustness: paradigms, mechanisms, and systems principles[J]. *Frontiers in genetics*, 2012, 3: 67.
- 11 Attwell D, Laughlin S B. An energy budget for signaling in the grey matter of the brain[J]. *Journal of Cerebral Blood Flow & Metabolism*, 2001, 21(10): 1133-1145.
- 12 Howarth C, Gleeson P, Attwell D. Updated energy budgets for neural computation in the neocortex and cerebellum[J]. *Journal of Cerebral Blood Flow & Metabolism*, 2012, 32(7): 1222-1232.
- 13 Cox D D, Dean T. Neural networks and neuroscience-inspired computer vision[J]. *Current Biology*, 2014, 24(18): R921-R929.
- 14 Bidaye S S, Bockemühl T, Büschges A. Six-legged walking in insects: how CPGs, peripheral feedback, and descending signals generate coordinated and adaptive motor rhythms[J]. *Journal of neurophysiology*, 2018, 119(2): 459-475.
- 15 Chen D, Peng P, Huang T, et al. Deep Reinforcement Learning with Spiking Q-learning[J]. *arXiv preprint arXiv:2201.09754*, 2022.
- 16 Black J E, Isaacs K R, Anderson B J, et al. Learning causes synaptogenesis, whereas motor activity causes angiogenesis, in cerebellar cortex of adult rats[J]. *Proceedings of the National Academy of Sciences*, 1990, 87(14): 5568-5572.
- 17 Dayan E, Cohen L G. Neuroplasticity subserving motor skill learning[J]. *Neuron*, 2011, 72(3): 443-454.
- 18 Kleim J A, Barbay S, Cooper N R, et al. Motor learning-dependent synaptogenesis is localized to functionally reorganized motor cortex[J]. *Neurobiology of learning and memory*, 2002, 77(1): 63-77.
- 19 Watkins C J C H, Dayan P. Q-learning[J]. *Machine learning*, 1992, 8(3): 279-292.
- 20 Sehne F, Osendorfer C, Rückstieß T, et al. Parameter-exploring policy gradients[J]. *Neural Networks*, 2010, 23(4): 551-559.
- 21 Schulman J, Wolski F, Dhariwal P, et al. Proximal policy optimization algorithms[J]. *arXiv preprint arXiv:1707.06347*, 2017.
- 22 Van Hasselt H, Guez A, Silver D. Deep reinforcement learning with double q-learning[C]//Proceedings of the AAAI conference on artificial intelligence. 2016, 30(1).
- 23 Wang Z, Schaul T, Hessel M, et al. Dueling network architectures for deep reinforcement learning[C]//International conference on machine learning. PMLR, 2016: 1995-2003.
- 24 Bellemare M G, Naddaf Y, Veness J, et al. The arcade learning environment: An evaluation platform for general agents[J]. *Journal of Artificial Intelligence Research*, 2013, 47: 253-279.
- 25 Mnih V, Badia A P, Mirza M, et al. Asynchronous methods for deep reinforcement learning[C]//International conference on machine learning. PMLR, 2016: 1928-1937.
- 26 Schulman J, Levine S, Abbeel P, et al. Trust region policy optimization[C]//International conference on machine learning. PMLR, 2015: 1889-1897.
- 27 Fujimoto S, Hoof H, Meger D. Addressing function approximation error in actor-critic methods[C]//International conference on machine learning. PMLR, 2018: 1587-1596.
- 28 Haarnoja T, Zhou A, Abbeel P, et al. Soft actor-critic: Off-policy maximum entropy deep reinforcement learning with a stochastic actor[C]//International conference on machine learning. PMLR, 2018: 1861-1870.
- 29 Maass W. Networks of spiking neurons: the third generation of neural network models[J]. *Neural networks*, 1997, 10(9): 1659-1671.
- 30 Zhang D, Zhang T, Jia S, et al. Recent Advances and New Frontiers in Spiking Neural Networks[J]. *arXiv preprint arXiv:2204.07050*, 2022.
- 31 O'Brien M J, Srinivasa N. A spiking neural model for stable reinforcement of synapses based on multiple distal rewards[J]. *Neural Computation*, 2013, 25(1): 123-156.
- 32 Yuan M, Wu X, Yan R, et al. Reinforcement learning in spiking neural networks with stochastic and deterministic synapses[J]. *Neural computation*, 2019, 31(12): 2368-2389.
- 33 Mahadevuni A, Li P. Navigating mobile robots to target in near shortest time using reinforcement learning with spiking neural networks[C]//2017 International Joint Conference on Neural Networks (IJCNN). IEEE, 2017: 2243-2250.
- 34 Doya K. Reinforcement learning in continuous time and space[J]. *Neural computation*, 2000, 12(1): 219-245.
- 35 Frémaux N, Sprekeler H, Gerstner W. Reinforcement learning using a continuous time actor-critic framework with spiking neurons[J]. *PLoS computational biology*, 2013, 9(4): e1003024.
- 36 Florian R V. Reinforcement learning through modulation of spike-timing-dependent synaptic plasticity[J]. *Neural computation*, 2007, 19(6): 1468-1502.
- 37 Frémaux N, Gerstner W. Neuromodulated spike-timing-dependent plasticity, and theory of three-factor learning rules[J]. *Frontiers in neural circuits*, 2016, 9: 85.

- 38 Bellec G, Scherr F, Subramoney A, et al. A solution to the learning dilemma for recurrent networks of spiking neurons[J]. *Nature communications*, 2020, 11(1): 1-15.
- 39 Kim J, Kwon D, Woo S Y, et al. On-chip trainable hardware-based deep Q-networks approximating a backpropagation algorithm[J]. *Neural Computing and Applications*, 2021, 33(15): 9391-9402.
- 40 Akl M, Sandamirskaya Y, Walter F, et al. Porting Deep Spiking Q-Networks to neuromorphic chip Loihi[C]//International Conference on Neuromorphic Systems 2021. 2021: 1-7.
- 41 Liu G, Deng W, Xie X, et al. Human-Level Control Through Directly Trained Deep Spiking Q-Networks[J]. *IEEE Transactions on Cybernetics*, 2022.
- 42 Patel D, Hazan H, Saunders D J, et al. Improved robustness of reinforcement learning policies upon conversion to spiking neuronal network platforms applied to Atari Breakout game[J]. *Neural Networks*, 2019, 120: 108-115.
- 43 Tan W, Patel D, Kozma R. Strategy and benchmark for converting deep q-networks to event-driven spiking neural networks[C]//Proceedings of the AAAI conference on artificial intelligence. 2021, 35(11): 9816-9824.
- 44 Tang G, Kumar N, Michmizos K P. Reinforcement co-learning of deep and spiking neural networks for energy-efficient mapless navigation with neuromorphic hardware[C]//2020 IEEE/RSJ International Conference on Intelligent Robots and Systems (IROS). IEEE, 2020: 6090-6097.
- 45 Zhang D, Zhang T, Jia S, et al. Population-coding and dynamic-neurons improved spiking actor network for reinforcement learning[J]. *arXiv preprint arXiv:2106.07854*, 2021.
- 46 Zhang D, Zhang T, Jia S, et al. Multiscale Dynamic Coding improved Spiking Actor Network for Reinforcement Learning[J]. 2022.
- 47 Seung S. *Connectome: How the brain's wiring makes us who we are*[M]. HMH, 2012.
- 48 Eichler K, Li F, Litwin-Kumar A, et al. The complete connectome of a learning and memory centre in an insect brain[J]. *Nature*, 2017, 548(7666): 175-182.
- 49 Takemura S, Aso Y, Hige T, et al. A connectome of a learning and memory center in the adult *Drosophila* brain[J]. *Elife*, 2017, 6: e26975.
- 50 Varshney L R, Chen B L, Paniagua E, et al. Structural properties of the *Caenorhabditis elegans* neuronal network[J]. *PLoS computational biology*, 2011, 7(2): e1001066.
- 51 White J G, Southgate E, Thomson J N, et al. The structure of the nervous system of the nematode *Caenorhabditis elegans*: the mind of a worm[J]. *Phil. Trans. R. Soc. Lond*, 1986, 314(1): 340.
- 52 Gaier A, Ha D. Weight agnostic neural networks[J]. *Advances in neural information processing systems*, 2019, 32.
- 53 Huttenlocher P R. Morphometric study of human cerebral cortex development[J]. *Neuropsychologia*, 1990, 28(6): 517-527.
- 54 Tierney A L, Nelson III C A. Brain development and the role of experience in the early years[J]. *Zero to three*, 2009, 30(2): 9.
- 55 Bruer J T. Neural connections: Some you use, some you lose[J]. *The Phi Delta Kappan*, 1999, 81(4): 264-277.
- 56 Dayan P, Abbott L F. Theoretical neuroscience: computational and mathematical modeling of neural systems[J]. *Journal of Cognitive Neuroscience*, 2003, 15(1): 154-155.
- 57 Akopyan F, Sawada J, Cassidy A, et al. Truenorth: Design and tool flow of a 65 mw 1 million neuron programmable neurosynaptic chip[J]. *IEEE transactions on computer-aided design of integrated circuits and systems*, 2015, 34(10): 1537-1557.
- 58 Davies M, Srinivasa N, Lin T H, et al. Loihi: A neuromorphic manycore processor with on-chip learning[J]. *Ieee Micro*, 2018, 38(1): 82-99.
- 59 Geweke J. Antithetic acceleration of Monte Carlo integration in Bayesian inference[J]. *Journal of Econometrics*, 1988, 38(1-2): 73-89.
- 60 Brockhoff D, Auger A, Hansen N, et al. Mirrored sampling and sequential selection for evolution strategies[C]//International Conference on Parallel Problem Solving from Nature. Springer, Berlin, Heidelberg, 2010: 11-21.
- 61 Salimans T, Ho J, Chen X, et al. Evolution strategies as a scalable alternative to reinforcement learning[J]. *arXiv preprint arXiv:1703.03864*, 2017.
- 62 Brockman G, Cheung V, Pettersson L, et al. Openai gym[J]. *arXiv preprint arXiv:1606.01540*, 2016.
- 63 Todorov E, Erez T, Tassa Y. Mujoco: A physics engine for model-based control[C]//2012 IEEE/RSJ international conference on intelligent robots and systems. IEEE, 2012: 5026-5033.
- 64 Achiam J. Openai spinning up[J]. GitHub, GitHub repository, 2018.
- 65 Kangin D, Pugeault N. On-policy trust region policy optimisation with replay buffers[J]. *arXiv preprint arXiv:1901.06212*, 2019.
- 66 Henderson P, Islam R, Bachman P, et al. Deep reinforcement learning that matters[C]//Proceedings of the AAAI conference on artificial intelligence. 2018, 32(1).
- 67 Rathi N, Roy K. DIET-SNN: A low-latency spiking neural network with direct input encoding and leakage and threshold optimization[J]. *IEEE Transactions on Neural Networks and Learning Systems*, 2021.
- 68 Horowitz M. 1.1 computing's energy problem (and what we can do about it)[C]//2014 IEEE International Solid-State Circuits Conference Digest of Technical Papers (ISSCC). IEEE, 2014: 10-14.

Appendix A The Hyper-parameter Configurations and Optimization Process of PPO

For each MuJoCo continuous control task, we ran 1e3 iterations, 1e3 steps per iteration, and a total of 1e6 steps of environment interaction. The deep policy network was trained in 25 epochs per iteration with a mini-batch size of 100, using Adam optimizer with a learning rate of 1e-5. The training configurations of the deep value network were the same as the deep policy network, but the learning rate was 1e-4. The discount factor γ for reward was 0.99, and the discount factor λ used in generalized advantage estimation was 0.95. The clip ratio ϵ_{clip} for PPO was 0.2. We presented the optimization process of PPO in Algorithm A1.

Algorithm A1 The optimization process of PPO.

- 1: Initialize deep policy network $\pi(\mathbf{a}|\mathbf{o})$ and deep value network $V(\mathbf{o})$ with parameter ϕ_π and ϕ_V .
- 2: **for** $iter = 1$ to $1e3$ **do**
- 3: Run π_{ϕ_π} to collect a set of episodes $\mathcal{D} = \{\epsilon^k\}$ containing $|\mathcal{D}|$ episodes, each ϵ^k is a episode contain $|\epsilon^k|$ data (samples or steps), $\epsilon^k := \{(\mathbf{o}^{k,t}, \mathbf{a}^{k,t}, r^{k,t+1}, \mathbf{o}^{k,t+1})\}$, $t \in [|\epsilon^k|]$.
- 4: Compute cumulative reward $R^{k,t}$ for each step t in every episode k using discount factor γ .
- 5: Update deep value network by minimizing the mean-square error:

$$\phi_V \leftarrow \arg \min_{\phi_V} \frac{1}{\sum_k |\epsilon^k|} \sum_{\epsilon^k \in \mathcal{D}} \sum_{t=0}^{|\epsilon^k|} (V(\mathbf{o}^{k,t}) - R^{k,t})^2$$
- 6: Estimate advantage $A^{k,t}$ for each step t in every episode k using generalized advantage estimation and deep value network $V_{\phi_V}(\mathbf{o})$.
- 7: Update the deep policy network by minimizing the following objective (the minimization is solved using Adam optimizer):

$$\phi_\pi \leftarrow \arg \min_{\phi'_\pi} \frac{1}{\sum_k |\epsilon^k|} \left[\sum_{\epsilon^k \in \mathcal{D}} \sum_{t=0}^{|\epsilon^k|} \min(r_{\phi'_\pi}(\mathbf{a}^{k,t}|\mathbf{o}^{k,t})A^{k,t}, g(r_{\phi'_\pi}(\mathbf{a}^{k,t}|\mathbf{o}^{k,t}))A^{k,t}) \right]$$

where $r_{\phi'_\pi}(\mathbf{a}^{k,t}|\mathbf{o}^{k,t}) := \frac{\pi_{\phi'_\pi}(\mathbf{a}^{k,t}|\mathbf{o}^{k,t})}{\pi_{\phi_\pi}(\mathbf{a}^{k,t}|\mathbf{o}^{k,t})}$, $g(r) := \text{clip}(r_{\phi'_\pi}(\mathbf{a}^{k,t}|\mathbf{o}^{k,t}), 1 - \epsilon_{\text{clip}}, 1 + \epsilon_{\text{clip}})$.

- 8: **end for**
 - 9: **Return:** Final learned deep policy network.
-

Appendix B The Forward Inference Pseudocode of Our SPN

Algorithm B1 The forward inference pseudocode of our SPN

- 1: Synaptic weight matrices \mathbf{W}^1 and \mathbf{W}^2 for middle processing and motor layer (randomly initialized and fixed);
 - 2: Score matrices corresponding to synaptic connections \mathbf{C}^1 and \mathbf{C}^2 for middle processing and motor layer (tuned by GA);
 - 3: Initialize the score threshold s_{th} ;
 - 4: Obtain the mask of synaptic connection $\mathbf{X}^1 = (\text{sigmoid}(\mathbf{C}^1) \geq s_{th})$ and $\mathbf{X}^2 = (\text{sigmoid}(\mathbf{C}^2) \geq s_{th})$ for middle processing and motor layer;
 - 5: Initialize the potential decay factor g and firing threshold v_{th} ;
 - 6: n -dimensional state observation, \mathbf{o} ;
 - 7: **for** $\tau = 1$ to T' **do**
 - 8: $\mathbf{v}_\tau^1 = g\mathbf{v}_{\tau-1}^1(1 - \mathbf{s}_{\tau-1}^1) + (\mathbf{W}^1 \times \mathbf{X}^1)\mathbf{o}$;
 - 9: $\mathbf{s}_\tau^1 = \mathbf{v}_\tau^1 > v_{th}$;
 - 10: $\mathbf{v}_\tau^2 = g\mathbf{v}_{\tau-1}^2 + (\mathbf{W}^2 \times \mathbf{X}^2)\mathbf{s}_\tau^1$;
 - 11: **end for**
 - 12: Generate output action, a ;
 - 13: **if** Continuous action space **then**
 - 14: $\mathbf{a} = \max_{1 \leq \tau \leq T'} \mathbf{v}_\tau^2$;
 - 15: **else**
 - 16: $a = \arg \max(\max_{1 \leq \tau \leq T'} \mathbf{v}_\tau^2)$;
 - 17: **end if**
-

Appendix C The Pseudocode for Our GA Version

Algorithm C1 The optimization process of our GA version

Input: number of total generations G , population size N , standard deviation of perturbations σ , ratio of truncation selection η , and fitness score function F .

Output: Elites = [] (store the elite of each generation).

for $i = 0, \dots, G-1$ generations **do**

 Create i generation population of N individuals \mathcal{P}^i .

for $j = 0, \dots, N-1$ individuals **do**

if $i = 0$ **then**

Initialization. $\theta_j^{i=0} = \sigma\epsilon$ or $-\sigma\epsilon$, $\epsilon \sim \mathcal{N}(\mathbf{0}, \mathbf{I})$ {initialize scores corresponding to all synaptic connections of SPN.}

else

Varying. $\theta_j^i = \theta_{j\eta}^{i-1} + \sigma\epsilon$ or $-\sigma\epsilon$, $j = 0, \dots, N-1$, $\theta_{j\eta}^{i-1} \in \mathcal{P}_\eta^{i-1}$. {Mutation.}

end if

Evaluation. $F_j = F(\theta_j^i)$ {Obtain the sub-network of SPN by sigmoid normalization of connection scores and filtering by score threshold. Based on the interaction between the sub-network and environment, obtain an episode and use its return as the fitness score.}

end for

Ranking. Sort θ_j^i with descending order by F_j

 Perform truncation selection with a ratio of η to produce the next generation's parents \mathcal{P}_η^i .

 Set elite candidates for generation i (top 10):

$C^i \leftarrow \theta_{1\dots 10}^i$.

 Select elite for generation i :

$\text{elite}^i \leftarrow \arg \max_{\theta \in C^i} \frac{1}{10} \sum_{k=1}^{10} F(\theta)$.

 Elites += [elite ^{i}]

end for

Return: Elites
